

Clay and pyrite transformations during ignition of pulverised coal*

F. H. HUBBARD AND R. J. MCGILL

Department of Geology, University of Dundee

AND

R. K. DHIR AND M. S. ELLIS

Department of Civil Engineering, University of Dundee

ABSTRACT. Clay minerals are the principal reactive, non-combustible, phases present in the pulverized coal burned in power station furnace units. Despite the short heating time involved, the clay mineral impurity is wholly transformed in the ignition.

Illitic clays are partially melted, fluxed by water and potash, to produce an aluminosilicate melt phase. The melt is frothed by the synchronous production of carbon dioxide in an iron oxide catalysed oxidation of associated carbonaceous matter. This produces the hollow, gas-filled, glass-walled spheres (cenospheres) characteristic of pulverized fuel ash (PFA). Partial, primary devitrification crystallization of mullite and quartz from the high-alumina glass is general and the extent of devitrification may influence the pozzolanic efficiency of the PFA cenospheres.

Without the advantage of potash fluxing, the kaolinite lattices are dehydrated and transformed, without melting, to amorphous aluminosilicate and crystalline mullite.

Oxidation of pyrite leads to coating of cenospheres by condensed magnetite and the emission of sulphur dioxide in the flue gases.

IN modern solid-fuel power stations steam is raised by burning finely crushed coal injected in a stream of pre-heated air at high speed into a furnace. Ignition in suspension is instantaneous at a temperature of *c.* 1500 °C (CEGB, 1972). A fine ash is produced (PFA—pulverized fuel ash) from the non-combustible mineral impurity of the coal (dominantly quartz, clay minerals, sulphides and oxides of iron, and some carbonates). The flash-ignition induces time-constrained thermal metamorphism and anatexis of the mineral impurity suite. The main component of PFA is an aluminosilicate glass in the form of hollow spheres (cenospheres). The pozzolanic properties of this material have led to the use of PFA as a partial substitute for cement in concrete manufacture. The control

of PFA compositional variation on pozzolanic activity is currently under investigation. Establishment of the nature and distribution of the ash components has yielded information on the mechanisms involved in the mineral transformations during ignition.

The major components of PFA

Fig. 1 shows a powder X-ray diffractogram obtained from a typical bulk ash. The major mineral phases indicated as present are quartz, mullite, hematite, and magnetite. The marked 'amorphous bulge' between *c.* 10° and 40° 2θ is characteristic. In addition to the glass cenospheres, SEM and TEM investigations have identified further amorphous components in irregular, sometimes skeletal, masses.

Quartz occurs as discrete grains whose morphological features suggest detrital grains which have

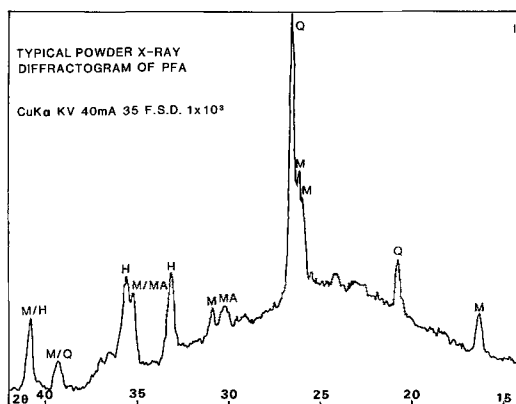


FIG. 1. X-ray powder diffractogram of PFA. Q = quartz, M = mullite, MA = magnetite, H = hematite.

* Read on 27 April 1983.

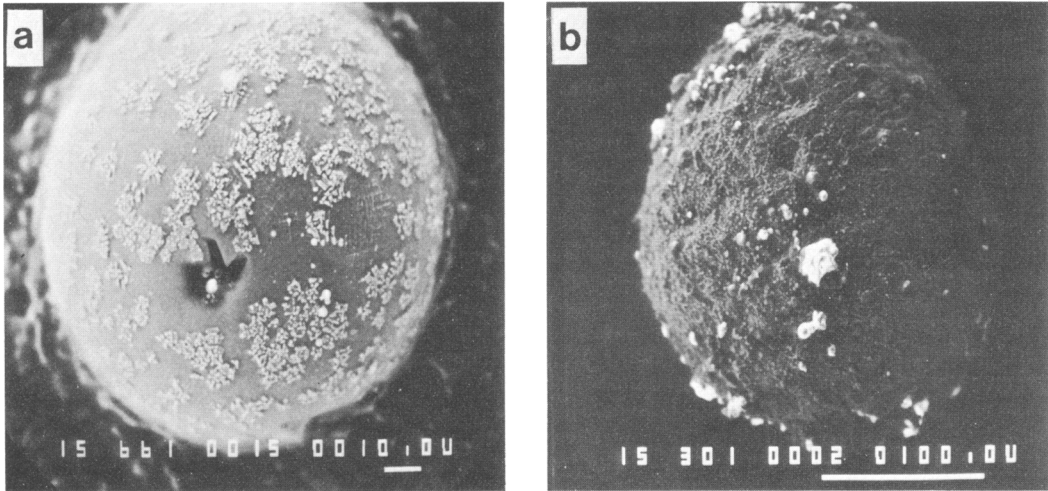


FIG. 2 (a) A cenosphere partially coated with well-crystallized magnetite. (b) Magnetite-encrusted cenosphere.

survived the ignition. XRD examination of isolated cenospheres has shown that quartz also occurs as a cryptocrystalline phase in the glass.

Mullite. Despite a careful search, mullite was not found in discrete grains in any of the ashes examined. Its two main modes of occurrence are as cryptocrystalline components in the cenospheric glass and in clay residues.

Hematite occurs in all ashes as irregular grains and aggregates which are probably relict from the coal impurity mineral suite.

Magnetite is found as partial or complete mantles on cenospheres (fig. 2a and b) and is thus a neocrystallization formed in the ignition event.

The amorphous components. The hollow glassy sphere component is volumetrically dominant over the irregular aggregates. The cenospheres occur in a wide size range, from a few microns diameter to as much as 1 mm. The smaller cenospheres are normally transparent (when free from magnetite) but are commonly opalescent in the larger size ranges. SEM examination showed that the cenosphere walls may be highly vesicular in the larger cenospheres (fig. 3a). Composite spheres (pleuro-spheres) are not uncommon with smaller spheres attached to the exterior and/or interior walls.

The amorphous aggregates have a relict platy habit (fig. 3b) and may be skeletal (fig. 4b). Some

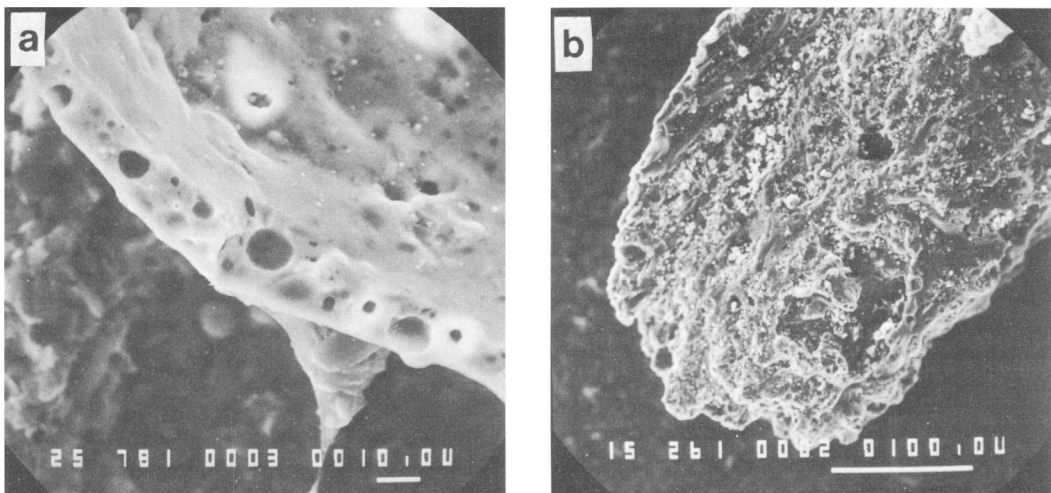


FIG. 3 (a) Vesicular wall of a cenosphere. (b) Residual amorphous residue after anatexis of clay.

have adhering small cenospheres (fig. 4a), and are residua from the anatexis of illite. Others, metamorphic derivatives of kaolinite, are free of cenospheres but include cryptocrystalline mullite.

Analytical methods

X-ray diffraction. Powder X-ray diffraction was used to identify the crystalline components present in the ashes. Ash samples were crushed in a tungsten carbide planetary ball-mill for thirty minutes before back-packing against glass in standard sample holders for a Philips automatic sample changer. The samples were analysed using Cu-K α radiation at 40 kV 30 mA on a Philips PW 1050 diffractometer fitted with a curved-graphite monochromator. Pulse height selection was used.

X-ray diffraction modal analysis was achieved by preparing suites of spiked ash samples by the addition of known weights of mullite, quartz, hematite, and magnetite to the same ash base. The mullite 16.45° 2 θ , the quartz 20.85° 2 θ , the magnetite 30.13° 2 θ , and the combined magnetite/hematite 62.5° 2 θ Cu-K α reflections were used for calibration. Intensities were measured in terms of half peak height width \times height above interpolated background. The amorphous contents were calculated by difference from 100. Reproducibilities of ± 2 wt. % mullite, ± 1 wt. % quartz and magnetite and ± 4 wt. % hematite and magnetite at the 95% confidence level were achieved.

A limited number of single cenospheres were examined by flat-film X-ray diffraction which revealed the presence of crystalline mullite and quartz.

X-ray fluorescence analysis. The bulk compositions of the ashes were determined by X-ray fluorescence procedures using a Philips PW 1410 sequential analyser with a Rh-target tube. 'Standard ashes' were prepared by analysing multiple fused pellets, prepared from two ashes, against similarly prepared international rock standards (W1, G2, and NIM-G). Analysis runs were made with the

unknown and standard ashes prepared as pressed powder pellets.

Loss on ignition. The residual coal contents of the ashes were determined by ignition of dry ashes at 900°C for thirty minutes.

TEM thin-film microanalysis. Aliquots of crushed ash were suspended in acetone and allowed to settle. A drop of the apparently clear supernatant liquid was transferred to a carbon-coated nylon grid and allowed to evaporate. The grid plus its load was then recoated with carbon. This procedure provided a well-dispersed sample with a high frequency of particles with edges fulfilling the thin-film criteria (Cliff and Lorimer, 1975). The samples were analysed using a modified AEI EM6G transmission electron microscope coupled to a Links System Model 290 analyser and Kevex energy-dispersive detector. Compositions were calculated from the equation:

$$\frac{C_X}{C_{Si}} = K_{X-Si} \frac{I_X}{I_{Si}}$$

where I_{Si} and I_X are simultaneously recorded K α characteristic X-ray intensities and C_{Si} and C_X the weight fraction of the elements Si and X in the thin film. A set of element proportionality constants (K_{X-Si}) was predetermined for the equipment using silicate mineral standards (McGill and Hubbard, 1981). Peak interference and background corrections were made by computer methods. Element loss in the electron beam was found to be negligible for the PFA components.

The composition of PFA and its components

The X-ray fluorescence spectrometric analysis of a wide range of ashes from UK sources showed there to be a very restricted compositional range. A typical major oxide analysis is shown in Table I with the corresponding modal analysis. The major

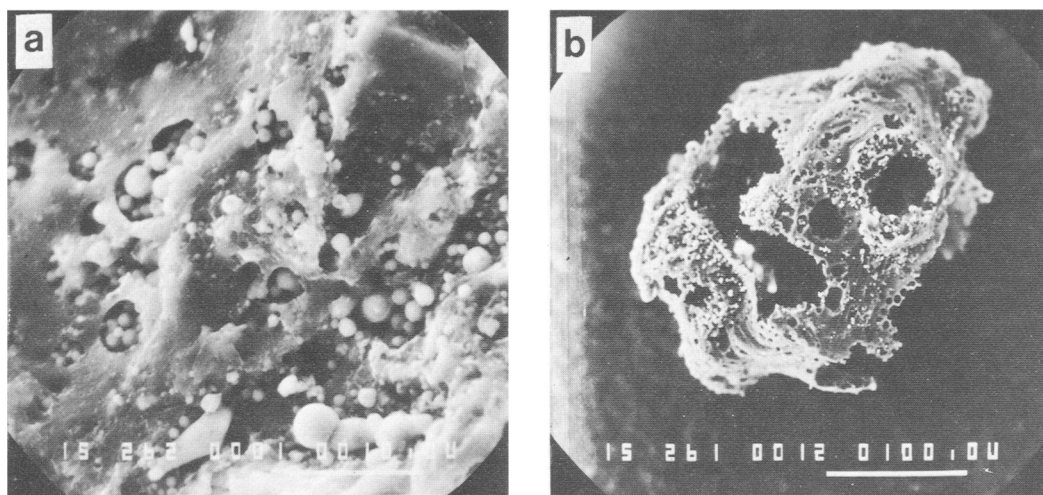


FIG. 4 (a) Minute cenospheres adhering to clay residue of fig 3b. (b) A skeletal, exhausted, clay residue.

TABLE I. Analytical Data for Ash P5 (wt%)

	SiO ₂	TiO ₂	Al ₂ O ₃	Fe ₂ O ₃ ⁽¹⁾	MgO	CaO	K ₂ O	MnO	SO ₃	L.O.I.
Bulk Ash ⁽²⁾	50.1	1.1	26.4	9.3	2.0	2.6	2.7	0.1	(4)	4.07
Cenospheres ⁽³⁾ n = 8	47.9	0.8	37.5	2.5	1.4	n.d.	9.0	n.d.	1.0	n.a.
	± 1.0	± 0.6	± 1.2	± 1.1	± 1.2		± 0.6		± 1.0	
Amorphous ⁽³⁾ Residua	65.6	1.2	17.8	5.7	1.6	3.5	2.3	0.1	2.1	n.a.
		Quartz	Mullite	Magnetite	Hematite	Amorphous	Carbon			
Ash Modal Analysis		3.6	14.2	6.7	8.3	63.1	4.1			

(1) Total iron calculated at Fe₂O₃.

(2) XRF analysis.

(3) TEM microanalysis.

(4) Included in L.O.I.

n.d. = not detected.

n.a. = not analysed.

variation noted was in the relative proportions of mullite, quartz, and amorphous component. Both quartz and mullite have significant negative coefficients of correlation (> -0.8) with the amorphous component and positive correlations with each other. These relationships reflect the variation of the cryptocrystalline quartz and mullite proportions in the cenospheres. Abnormal mullite contents as high as 40% have been obtained but most ashes assay within a band of 10–20 wt. % mullite.

The amorphous components were analysed by the TEM thin-film microanalysis procedures. The cenosphere compositions remained fairly consistent within any one ash. The data in Table I show the compositional range derived from the eight analyses of cenospheres from one ash. There is some more significant variation between ashes (Table II), mainly in the relative proportions of K₂O and SiO₂, but a general hyperaluminous silicate melt composition is maintained. The ceno-

TABLE II. TEM Microanalytical Data for Cenospheres.

Normalised on a Water-free Basis

Ash	n	SiO ₂	Al ₂ O ₃	Fe ₂ O ₃ ⁽¹⁾	MgO	K ₂ O	TiO ₂	SO ₃
P 1	3	48.76	36.90	2.34	1.97	8.78	0.95	1.62
P 2	3	49.45	37.19	2.22	1.51	9.57	0.35	0.72
P 4	6	49.12	37.05	1.94	1.26	9.67	0.84	1.94
P 5	8	47.86	37.45	2.53	1.42	9.00	0.79	0.96
P 9	4	47.89	36.37	2.59	2.40	9.57	0.64	0.54
P11	3	48.02	37.04	2.47	1.49	9.83	0.72	0.42
P12	2	48.38	37.27	2.07	1.95	8.49	0.89	1.40
P13	3	54.14	34.81	2.92	2.24	4.69	1.38	0.57
P14	1	52.00	37.18	2.95	1.95	3.76	1.40	0.77
P24	3	56.86	30.18	4.61	2.25	4.01	1.44	0.66
\bar{X}	39	50.61	36.05	2.77	1.86	7.28	0.95	0.96
Raask \bar{X}		58.00	27.85	8.28	1.55	1.75	-	-

(1) Total iron calculated as Fe₂O₃

spheric material is characteristically aluminium enriched and calcium depleted compared with the bulk ash composition and is suitable to have been derived from the partial melting of a potash-bearing clay.

Less analytical data are available for the amorphous residua which are often difficult to isolate in a manner suitable for thin-film quantitative analysis (Table III). The anatectic residues have higher lime and lower alumina than the cenospheres. The cenosphere and residua compositions are such that they may respectively represent melt and refractory residuum from illite anatexis. The metamorphic aggregate composition (P12K in Table III) is that of a volatile-free kaolinite.

Discussion

The powdered coal and its impurities are abruptly elevated to high temperature for a very short period of time. Consequently reaction kinetics are a more significant controlling factor than thermodynamic equilibrium in the production of PFA. This is dramatically expressed in the preservation of unignited coal fragments in the ash.

Quartz and hematite survive the brief exposure to high temperature while pyrite is completely oxidized to magnetite with the release of sulphur dioxide. This is the major source of the sulphur dioxide of the flue gases which contributes to 'acid rain' pollution. The proportion of magnetite in the solid waste provides a measure of the pollutant emission from a particular coal in a particular furnace unit. Removal of the pyrite (SG 5) by a gravity separation procedure following the milling of the coal might prove an attractive alternative to flue gas 'scrubbing' with lime to precipitate the sulphur dioxide as gypsum.

The greatest changes are wrought in the clay fraction of the mineral impurity which is com-

pletely transformed. No clay peaks were identified in any of the PFA X-ray diffractograms. In progressive heating of clay minerals, loss of structural water and impurities in the 200–900 °C temperature range is followed by crystallization of mullite and cristobalite before melting at 1100–1600 °C. Because of the rapid heating in the furnace units, the clays in the pulverized coal are raised instantaneously to the melting temperature range. Bound water and potash released in the thermal destruction of the illite will flux partial melting. The melt is produced as a froth of gas-filled bubbles, the cenospheres, which are rapidly chilled. This partial melting takes place in varying degrees depending on such factors as the specific composition, purity, and fineness of the clay fraction as well as the local heating conditions and the time held within the melting temperature range particular to the furnace aggregate. The occurrence of pleuropheres suggests co-formation of glass bubbles of varying size, marking local irregularities of synchronous gas release. The vesicular walls of some of the larger cenospheres favour the view that gas and melt generation had a common focus of activity. The irregular masses of amorphous material, commonly with attached small cenospheres, suggest the source of the melt and the incompleteness of both the melting and the expulsion of the melt fraction from the refractory residuum.

Raask (1968) investigated cenospheres derived by flotation from PFA from a variety of power stations, i.e. intact, buoyant, gas-filled cenospheres. The major oxide compositions he obtained, by an unspecified procedure, differ from those obtained in this study where selected, uncontaminated, thin shards from individual cenospheres were analysed. Raask's analysis from four power stations show higher silica and iron oxide and lower alumina and potash concentrations than those obtained from TEM microanalysis of cenospheres from ten

TABLE III TEM Microanalytical Data for Amorphous Residua
Normalised on a Water-free Basis.

Ash	n	SiO ₂	Al ₂ O ₃	Fe ₂ O ₃ ⁽¹⁾	MgO	CaO	K ₂ O	TiO ₂	MnO	SO ₃
P 5	4	65.65	17.83	5.72	1.61	3.48	2.30	1.22	0.11	2.08
P13	2	64.08	17.86	6.69	3.31	2.25	2.62	0.95	-	0.52
P14	1	60.57	17.43	8.71	3.34	2.54	1.29	1.08	-	0.54
P12K	1	53.77	44.14	0.50	-	-	1.03	0.24	-	0.32

(1) Total iron calculated as Fe₂O₃.

sources in this investigation (Table II). The yield of cenospheres in flotation experiments carried out in the course of our study was markedly impure and, in particular, included a significant proportion of cenospheres with adhering magnetite and amorphous residuum. If Raask's analyses were made on bulked flotation samples, this may to some degree explain the differences in compositions found.

Raask (1968) determined the composition of the gas in the cenospheres by gas chromatography and found it to be mainly carbon dioxide and nitrogen with traces of carbon monoxide. He concluded that the gas evolved largely from oxidation of small amounts of carbonaceous matter catalysed by ferric oxide. Raask also showed that the cenospheres decrepitated on heating to 300 °C, presumably associated with the release of water dissolved in the glass. He did not specify the source of the cenospheric glass melt nor identify any amorphous residue.

The clay minerals most frequently found in coal are kaolinite and illite (Mackovsky, 1968). The relatively high levels of potash in the analysed cenospheres suggest that the parent clay mineral was illite (K_2O 5–6%) rather than kaolinite ($K_2O \sim 0\%$). Kaolinite has an extremely high ash-fusion point due to the absence of alkali. The lattices of any kaolinite originally present are wholly destroyed without melting to produce the mullite-bearing, cenosphere-free, amorphous aggregates. Illite may contain iron ($2K_2O \cdot MeO \cdot 8Al_2O_3 \cdot 24SiO_2 \cdot 12H_2O$ where $Me = Fe, Ca, Mg$) and some pyrite impurity is predictable. In the environment of the coal-seam the clay minerals will inevitably have intimately associated carbon, particulate and/or in clay-organic complexes. In the melting episode, water and potash released from the disintegrating illite lattices would act as fluxes allowing melting to proceed and would dissolve in the product aluminosilicate melt. The iron oxide and carbon in the active systems would provide gas generation 'at source' to froth and discharge the melt to produce cenospheres on cooling.

The localization of mullite and quartz within the cenospheric glass, indicated by this study, is significant. The most reactive component of PFA in cementation is likely to be the disordered glass. An

increased proportion of the crystalline components reduces the disorder and is likely to reduce the pozzolanic efficiency of the ash. These theoretical presumptions are currently under test. The crystallites of both quartz and mullite in the glass are small and apparently widely dispersed through the glass. Attempts to identify and locate the mineral phases by SEM back-scattered electron imaging proved unsuccessful. This suggests that the mullite and quartz represent maximum nucleation crystallization devitrification of the aluminosilicate glass, i.e. high temperature, primary devitrification at many nucleation sites but with low linear growth velocity. With glass formation restricted to a time measurable in milliseconds, postulation of intermediate crystallizations *en route* to melting seems insupportable on kinetic grounds. The rate of cooling through the glass transformation point in the flue gases is also high, in the order of 50 milliseconds, but seems, nevertheless, to have been sufficiently slow for quartz and mullite nucleation but only limited growth. The high alumina concentration in the melt may have stimulated local 'long-range' order in the glass to nucleate mullite ($3Al_2O_3 \cdot 2SiO_2$) with the localized resultant excesses of SiO_2 nucleating as quartz.

Acknowledgement. The research reported in this paper is part of a wider-ranging investigation of PFA and its use in concrete, sponsored by the Central Electricity Generating Board.

REFERENCES

- CEGB (1972) *PFA utilisation*. Central Electricity Generating Board.
- Cliff, G., and Lorimer, G. W. (1975) *J. Microsc.* **103**, 203.
- Mackovsky, M.-Th. (1968) In *Coal and Coal-bearing Strata* (D. Murchison and T. S. Westall, eds.). Oliver and Boyd, Edinburgh and London.
- McGill, R. J., and Hubbard, F. H. (1981) In *Quantitative Microanalysis with High Spatial Resolution* (G. W. Lorimer, M. Jacobs, and P. Doig, eds.). Metals Society, London, 30–4.
- Raask, E. (1968) *J. Inst. Fuel*, **41**, 339–44.

[Manuscript received 29 July 1983;
revised 5 September 1983]